Mine Water and the Environment (2024) 43:136–147
https://doi.org/10.1007/s10230-024-00975-5

TECHNICAL ARTICLE

Aquifer Water Abundance Evaluation Based on a Variable Weight Model

Aoshuang Mei[1] · Qiang Wu[1,2,3] · Keyao Han[4] · Yifan Zeng[1,2,3] · Pengfei Yang[5] · Yanping Miao[6] · Yang Lv[7] · Yashuai Cui[1] · Liang Yang[1]

Received: 30 August 2023 / Accepted: 12 February 2024 / Published online: 2 April 2024

Abstract

Existing aquifer water abundance evaluation methods employ fixed and constant index weights and overlook variations within major influencing factors as well as interactions among multiple factors. We propose a water abundance index method based on a variable weight model that considers various water abundance influencing factors and their respective weights, and quantitatively determines the weights of the same factor across different state values. This paper establishes a comprehensive system of four categories and 16 subcategories of main influencing factors that describe the distribution pattern of water abundance, considering lithological characters, hydraulic characteristics, structural factors, and geophysical parameters that influence aquifer water abundance. The variable weight model is used along with the K-means clustering method in dynamic clustering to determine the variable weight interval thresholds for each index of the main influencing factor. Additionally, we investigated the construction of the state variable weight vector, determination of weight adjustment parameters, quantitative assessment of the interaction relationship, and relative importance of each main influencing factor in relation to aquifer water abundance. Finally, an evaluation method and mathematical model for the water abundance index based on the variable weight model are developed. This study provides a detailed description of the specific implementation steps of the water abundance index method based on the variable weight model, using the direct water-filled $J_2z-^{\#}2$ coal seam roof fissured aquifer in the Xiaojihan coal mine as a case study. The evaluation results were then verified using drainage data from the working face. The findings indicate that a comparison with the traditional constant weight evaluation results demonstrates that the variable weight model better reflects the characteristics of aquifer heterogeneity and achieves higher prediction accuracy.

Keywords Analytic hierarchy process · The constant weight model · The variable weight model · Multisource information fusion · Mining · China

Introduction

Coal plays a crucial role as a primary energy source in China (Mu et al. 2022). In most mining areas in China, sandstone pore fissured aquifer s or loose pore aquifers are commonly found above the coal seam roof (Mei et al. 2023; Zeng et al. 2022). The mining of coal seams leads to the fracturing of the overburden rock, which in turn results in the occurrence of roof water inrush disasters—a significant water-related hazard encountered during mining operations (Gui and Lin

✉ Yifan Zeng
zengyf@cumtb.edu.cn

1 National Engineering Research Center of Coal Mine Water Hazard Controlling, China University of Mining and Technology, Beijing 100083, China

2 University of Mining and Technology (Beijing) Inner Mongolia Research Institute, Ordos 017000, Inner Mongolia, China

3 Key Laboratory of Mine Water Hazard Controlling, National Mine Safety Administration, Beijing 100713, China

4 Yellow River Institute of Eco-Environmental Research, Zhengzhou 450000, Henan, China

5 Xiaojihan Coal Mine, Shaanxi Huadian Yuheng Coal & Electricity Co., Ltd., Yulin 719000, Shaanxi, China

6 SHCCIG Shenmu Hongliulin Mining Co., Ltd., Shenmu 719300, Shaanxi, China

7 Shaanxi Shanmei Caojiatan Mining Co., Ltd., Yulin 719000, Shaanxi, China

2016). Coal seam roof water hazard occurs when mining-induced cracking intersects with a water-filled aquifer in an area characterized by high water abundance (Zeng et al. 2017). In other words, the aquifer serves as the material base for water inrush from the coal seam roof, and the water abundance within the aquifer directly influences the volume and duration of water inrush. The assessment of aquifer water abundance primarily involves geophysical exploration methods, and comprehensive prediction models that consider relevant factors through mathematical analysis (Li 2010; Qu et al. 2023; Wang 2011). Nevertheless, regardless of the type of geophysical exploration method employed, the assessment of aquifer water abundance can only provide qualitative evaluations of its relative strength. Therefore, utilizing comprehensive exploration data gathered during mining operations, including exploration activities, construction, and production processes for conducting near-quantitative or quantitative prediction research on the water abundance within the aquifer above the coal seam roof, holds immense importance in guiding efforts towards preventing and controlling coal mine roof water hazard in China.

Wu et al. (2014, 2015a, b, c) developed a comprehensive evaluation index system and weight determination method for assessing the water abundance of water-filled aquifers, which is known as the "water abundance index method." Subsequently, various comprehensive analysis methods for hydrogeologic factors have been derived and have gained widespread promotion and application in mining areas across China (Li et al. 2022b; Mei et al. 2023; Wu et al. 2015b; Zeng et al. 2017). Currently, various methods, including analytic hierarchy process (AHP), Bayes discriminant model, fuzzy analytic hierarchy process, and fuzzy clustering synthesis, are used to determine the weights of the evaluation indices (Han et al. 2012; He et al. 2019; Hou et al. 2019; Pang et al. 2022). Additional evaluation indicators, such as the degree of weathering, lithology combination index, sand-mud ratio, sand-mud interaction layer, lithology coefficient, and fractal dimension, have also been identified to replace the geologic structural factor index (Xiao et al. 2018; Xue 2020; Zhang et al. 2019). These methods have significantly contributed to the quantitative prediction and evaluation of the water abundance in water-filled aquifers above the coal seam roof, as well as the assessment of the risk of roof water hazard. However, the current evaluation index fusion follows a constant weight model where weights assigned to the main influencing factors remain unchanged throughout the evaluation process. This means that these weights do not adapt to changes in factor values. While traditional methods can describe the relative importance of the different indicators, they overlook variations within individual factors as well as interactions among multiple factors. This paper proposes a water abundance index method that utilizes a variable weight model. By examining the direct water-filled aquifers in the 11th and 13th panels of the Xiaojihan coal mine, we have demonstrated that the method can consider various water abundance influencing factors and their respective weights, while also quantitatively determining the weights of the same factor across different state values. The evaluation results are shown to be more accurate than the traditional constant weight model.

Study Area Conditions

Located in the inland northwest of China, the Xiaojihan coal mine is situated in Yulin City, Shaanxi Province. Most of the mine surface is covered by Quaternary sediments, with intermittent exposures of the Lower Cretaceous Luohe (K_1l) and Lower Jurassic Anding Formations (J_2a). From oldest to youngest, the strata comprise the Middle Jurassic Yan'an (J_2y), Zhiluo (J_2z), Anding (J_2a), the Lower Cretaceous Luohe (K_1l), the Middle Pleistocene Lishi (Q_2l), and the Upper Pleistocene Salawusu (Q_3s) Formations, along with the Holocene alluvial-diluvial (Q_4^{al+pl}), and aeolian sand (Q_4^{eol}) layers. The coal-bearing strata consist of the Middle Jurassic Yan'an Formation (J_2y), with the primary coal seam being the $^{\#}2$ coal. The mining operations encompass the 11th and 13th panels (Fig. 1). The Xiaojihan Mine exhibits a monocline structure trending northeast and northwest, characterized by an average dip angle of less than 1°. During exploration, well construction, and production processes, no significant fold structures or faults with a drop greater than 20 m were observed, and there were no indications of magmatic rock activity. The geologic structure was found to be relatively simple. The aquifer above the $^{\#}2$ coal seam in the Xiaojihan Mine can be classified into several categories: the J_2z–$^{\#}2$ coal seam roof fissured aquifer, the J_2a fissured aquifer, the K_1l pore-fissured aquifer, and the Quaternary pore aquifer. The aquiclude primarily consists of Q_2l loess, underlain by mudstone and siltstone in the bedrock. Based on the exploration data, the primary water-filled aquifer for mining the $^{\#}2$ coal seam is the J_2z–$^{\#}2$ coal seam roof fissured aquifer. The specific capacity ranges from 0.01 to 0.037 L/s·m, and the hydraulic conductivity ranges from 0.0208 to 0.1318 m/d. However, the aquifer exhibits low water abundance.

Materials and Methods

Water Abundance Index Method

Determine the Impact Indicators

Aquifer water abundance refers to the capacity of rock strata to provide water, which is primarily determined by aquifer

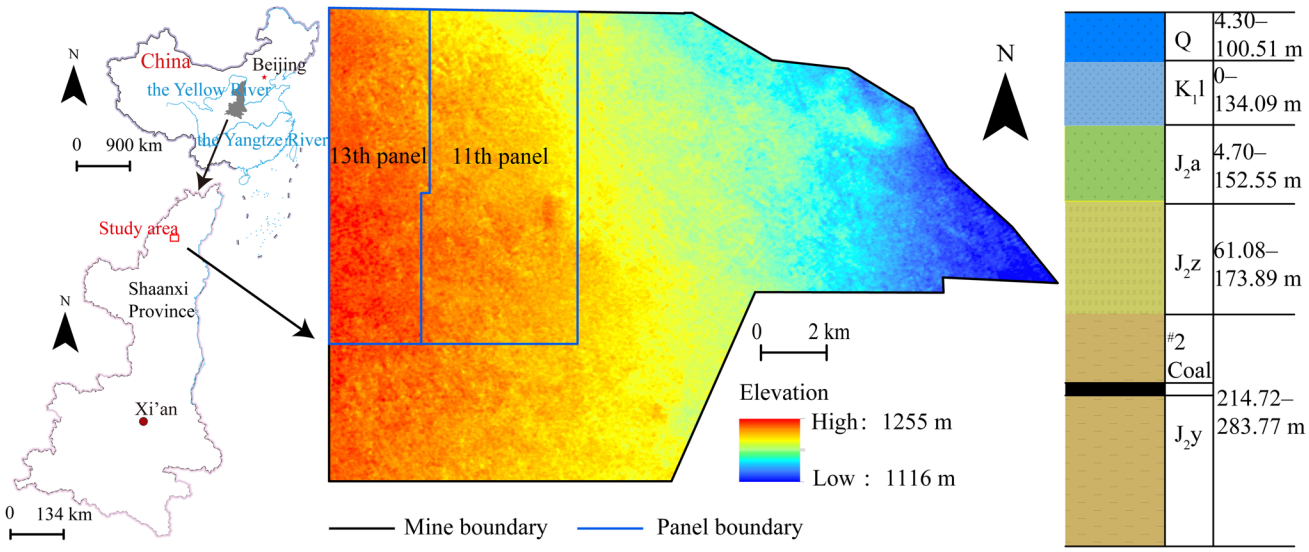

Fig. 1 Location of the study area

recharge, storage capacity, and water conductivity. The classification of aquifer water abundance is provided by the 'Coal Mine Water Control Rule's based on the specific capacity of boreholes. Though this method is concise, it only provides a point evaluation (National Coal Mine Safety Administration 2018). By systematically analyzing the lithological characters, hydraulic characteristics, geologic structural factors, and geophysical parameters of the aquifer (Li et al. 2022a, 2022b; Wu et al. 2015a), an index system for evaluating the water abundance of the aquifer was developed. This system consists of four categories and sixteen sub-categories, including the aquifer thickness, ratio of brittle and plastic rock, core recovery rate, specific capacity, hydraulic conductivity, flushing fluid consumption, spring flow, groundwater runoff modulus, geologic structure (faults, collapse columns, and folds, etc.), integrity coefficient, resistivity, apparent polarizability, half-life, attenuation, and more, as depicted in Fig. 2. Due to limitations in data type and accuracy within the study area, five indicators were selected for the analysis of water abundance zoning, namely the aquifer thickness, ratio of brittle and plastic rock, core recovery rate, specific capacity, and hydraulic conductivity.

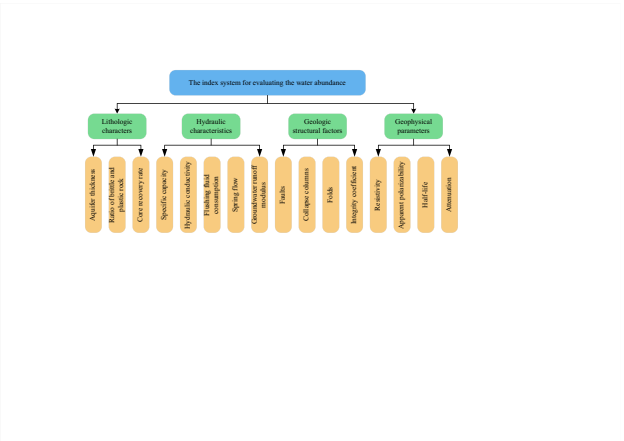

Fig. 2 Index system for evaluating the water-abundance

Standardization of Index Values and Making Them Dimensionless

To address the disparity in units and measurements of the main influencing factor index values in the model, it is necessary to standardize these values and make them dimensionless using the range standardization method. In this method, incentive indices (which means the higher the index values, the greater the water abundance) use the maximum value method (Eq. 1), while punitive indices utilize the minimum value method (Eq. 2; Zeng 2018).

$$Y_{\mathrm{i}} = \frac{y_i - y_{\min}}{y_{\max} - y_{\min}} \tag{1}$$

$$Y_{\mathrm{i}} = \frac{y_{\max} - y_i}{y_{\max} - y_{\min}} \tag{2}$$

where Y_i is the index value of the influencing factors after being made dimensionless at point i; y_i is the quantitative index value of the influencing factors at point i; y_{max} is the maximum quantitative index value of influencing factors in the study area; and y_{min} is the minimum quantitative index value of the influencing factors in the study area.

Water Abundance Evaluation of Aquifers

Utilizing GIS's spatial information processing and analysis capabilities, the primary factors influencing the water abundance of aquifers and their respective weights are coupled. Building on information fusion, an aquifer water abundance evaluation model is developed (Eq. 3), introducing the initial water abundance index (WI) to assess the aquifer water abundance. Subsequent to establishing the initial water abundance index model, information processing and analysis of each thematic map is conducted, employing a frequency histogram to statistically analyze the water abundance index values for each block. By conducting additional fitting analysis and inverse identification of known points, the threshold for water abundance evaluation zoning is ultimately determined. Subsequently, the aquifer is divided into water abundance evaluation zones based on this threshold, resulting in the generation of an aquifer water abundance evaluation zoning map.

$$WI = \sum_{i=1}^{n} W_i \bullet f_i(x, y) \tag{3}$$

where WI is the water abundance index; W_i is the weight of influencing factors; f_i is a single factor influence value function; x and y are geographical coordinates; and n is the number of influencing factors.

Analytic Hierarchy Process (AHP)

The AHP is a decision-making method that breaks down the elements associated with decision-making into hierarchical levels, including target level, sub-criteria level, and decision-making level. It then performs qualitative and quantitative analysis based on this structure. The specific calculation steps of AHP are as follows: (1) establish a hierarchical structure model; (2) form a judgment matrix based on pairwise comparisons using the nine importance levels and assignments provided by Saaty (Saaty 1990). The scale of the judgment matrix is represented in Eq. 4. (3) Perform hierarchical single ranking and conduct a consistency test. The calculation formulas for the consistency index (CI), random consistency index (RI), and consistency ratio (CR) are presented in Eq. 5.

$$a_{ij} = \frac{1}{a_{ji}} \tag{4}$$

where α_{ij} is the judgment matrix element and the scaling method is shown in Table 1.

Table 1 Proportion scale table

Ratio of factor i to factor j	Quantized value
Equally important	1
Slightly important	3
Relatively strongly important	5
Strongly important	7
Extremely important	9
The intermediate value of two adjacent judgments	2,4,6,8

$$\begin{cases} CI = \dfrac{\lambda - m}{m - 1} \\ RI = \dfrac{CI_1 + CI_2 + \cdots + CI_m}{m} \\ CR = \dfrac{CI}{RI} \end{cases} \tag{5}$$

where CI is the consistency index, λ is the maximum eigenvalue of the judgment matrix; m is the order of the judgment matrix; RI is a random consistency index; and CR is the consistency ratio. If CR < 0.1, the judgment matrix passes the consistency test; otherwise, it does not have satisfactory consistency.

The AHP method is used to determine the weights of the influencing factors, and the water abundance index is computed using Eq. 6.

$$WI = \sum_{i=1}^{n} W_{AHPi} \bullet f_i(x, y) \tag{6}$$

where W_{AHPi} is the constant weight determined by the AHP method after satisfying the consistency test.

Variable Weight Theory

The concept of variable weight emphasizes the continuous modification and adjustment of weight values based on the spatial positions and temporal durations of the specific decision-making process, accounting for potential significant changes (Wang 1985). The variable weight model addresses the flawed notion of fixed weights for each factor in the constant weight model. It mitigates the impact of a single factor being nullified by other factors during mutations, resulting in more realistic evaluation outcomes (Li and Hao 2009; Wang et al. 2014; Yu et al. 2022). The specific approach for determining the variable weights of the index follows.

Constructing the State Variable Weight Vector

The precise construction of the state variable weight vector is crucial for ensuring the reliability of the prediction results. Based on an analysis of the variable weight evaluation characteristics of the water abundance in the direct water-filled

aquifer of J_2z–$^{\#}2$ coal seam roof fissure, this study introduces two approaches, namely 'incentive' and 'punishment', to effectively promote or impede the main influencing factors of the roof aquifer water abundance. This approach accurately captures the effect of sudden changes in the index values of each main influencing factor on the evaluation results, while ensuring that the intensity of 'incentive' outweighs that of 'punishment'. Building on the aforementioned analysis, this paper establishes the mathematical formula for the state variable weight vector of the aquifer water abundance for the same factor (Eq. 7). The corresponding curve of the state variable weight vector for the same factor is depicted in Fig. 3.

$$W_j(x)\begin{cases} e^{\alpha_1(d_{j1}-x)}+c-1, x\in[0,d_{j1}) \\ c, x\in[d_{j1},d_{j2}) \\ e^{\alpha_2(x-d_{j2})}+c-1, x\in[d_{j2},d_{j3}) \\ e^{\alpha_3(x-d_{j3})}+e^{\alpha_2(d_{j3}-d_{j2})}+c-2, x\in[d_{j3},1) \end{cases} \tag{7}$$

where c, α_1, α_2, and α_3 are the weight adjustment parameters and d_{j1}, d_{j2}, and d_{j3} are the j^{th} factor variable weight interval thresholds.

The variable weight interval threshold d_{j1}, d_{j2}, d_{j3} divides the state value of the same factor into four intervals: $[0,d_{j1})$ belongs to the punishment interval; $[d_{j1},d_{j2})$ belong to the invariant interval; $[d_{j2},d_{j3})$ belongs to the initial incentive interval; and $[d_{j3},1]$ belongs to the strong incentive interval.

Determining the Variable Weight Interval of the Main Influencing Factors

The data of each main influencing factor is classified using the K-means clustering method. The classification category is determined as four categories based on the requirements of the state variable weight vector. According to the classification results, the critical classification values of each main influencing factor index value (f_{j1}, f_{j2}, f_{j3}, f_{j4}, f_{j5}, f_{j6}) are determined, and the variable weight interval threshold of each factor is calculated by Eq. 8.

$$\begin{cases} d_{j1}=\dfrac{(f_{j1}+f_{j2})}{2} \\ d_{j2}=\dfrac{(f_{j3}+f_{j4})}{2} \\ d_{j3}=\dfrac{(f_{j5}+f_{j6})}{2} \end{cases} \tag{8}$$

where d_j is the variable weight interval threshold of jth factor; f_j is the classification critical value of the index value of the jth factor in the clustering classification.

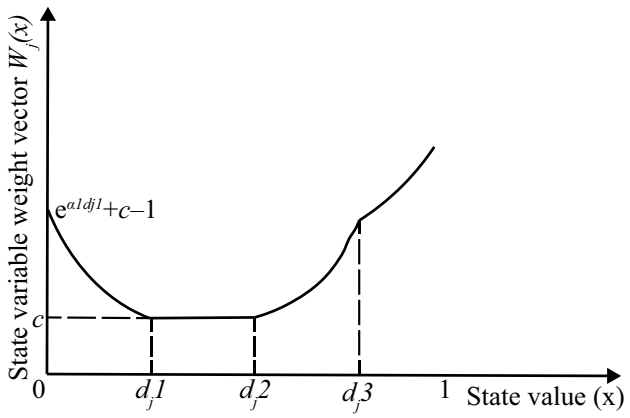

Fig. 3 Graph of state variable weight vector

Solving Model Parameters

The parameters of the variable weight model have control and adjustment effects on the variable weight effect. Due to the limited research on determining the model parameters at present, this paper proposes a method to determine the weight adjustment parameters in the variable weight evaluation model for aquifer water abundance, aiming to achieve the desired weight adjustment effect. The following steps are followed: using five main influencing factors as an example, first determine the constant weight for each factor (w_1^0, w_2^0,…, w_5^0); next, select a specific evaluation unit and assign factor index values x_1, x_2, x_3, and x_4 to different variable weight intervals, while x_5 is assigned to the punishment interval. Finally, determine the ideal variable weight weights (w_1, w_2,…, w_5) for the main influencing factors of the evaluation unit, along with the parameters a_1, a_2, a_3, and c. The solution formula is as follows:

$$\begin{aligned} \alpha_1&=\frac{1}{d_{11}-x_1}\ln\left[\frac{w_1w_2^0-w_2w_1^0}{w_2w_1^0}c+1\right] \\ \alpha_2&=\frac{1}{x_3-d_{32}}\ln\left[\frac{w_3w_2^0-w_2w_3^0}{w_2w_3^0}c+1\right] \\ \alpha_3&=\frac{1}{x_4-d_{43}}\ln\left[\frac{w_4w_2^0-w_2w_4^0}{w_2w_4^0}c\right. \\ &\left.+2-\left(\frac{w_3w_2^0-w_2w_3^0}{w_2w_3^0}c+1\right)^{\frac{d_{43}-d_{42}}{x_3-d_{32}}}\right] \end{aligned} \tag{9}$$

$$\begin{cases} k_1 = \dfrac{w_2^0 - w_2^0(w_1 + w_2 + w_3 + w_4) - w_2 w_5^0}{w_2 w_5^0} \\ k_2 = \dfrac{w_1 w_2^0 - w_2 w_1^0}{w_2 w_1^0} \\ k_3 = \dfrac{d_{51} - x_5}{d_{11} - x_1} \\ k_1 c = (k_2 c + 1)^{k_3} - 1 \end{cases} \tag{10}$$

x_1, x_2, x_3,… x_n are factor index values; d_{12}, d_{13}, d_{21}, d_{22}, d_{23},… d_{n1}, d_{n2}, d_{n3} are variable weight interval thresholds; w_1^0、w_2^0、w_3^0…w_n^0 are constant weight values of the factor; and w_1、w_2、w_3、…w_n are variable weight values of factors.

Determine the Variable Weight

The partition variable weight model is employed to determine the variable weight of each main influencing factor. This is achieved by constructing the state variable weight vector, dividing and establishing the weight adjustment interval and threshold, as well as solving for the weight adjustment parameters. The mathematical expression for this model can be seen in Eq. 11.

$$W(x) \triangleq \frac{W_0 S(X)}{\sum_{j=1}^{m} W_j^0 S_j(X)} \triangleq \left(\frac{W_1^0 S_1(X)}{\sum_{j=1}^{m} w_j^0 S_j(X)}, \frac{W_2^0 S_2(X)}{\sum_{j=1}^{m} w_j^0 S_j(X)}, \cdots, \frac{W_m^0 S_m(X)}{\sum_{j=1}^{m} w_j^0 S_j(X)} \right) \tag{11}$$

where S(X) is m dimensional partition state variable weight vector; $W_0 = \left(w_1^0, w_2^0, \cdots w_m^0\right)$ is any constant weight vector; and $W(X)$ is m dimensional partition variable weight vector.

Using Eq. 12 to calculate the water abundance index based on the variable weight model:

$$WI = \sum_{i=1}^{m} Wvwmi \bullet f_i(x, y) = \sum_{i=1}^{m} \frac{W_i^{(0)} S_i(X)}{\sum_{j=1}^{m} w_j^{(0)} S_j(X)} \bullet f_i(x, y) \tag{12}$$

where w_{VWMi} is variable weight vector of influencing factors; $w^{(0)} is$ any constant weight vector; and $S_j(X)$ is m-dimensional partition state variable weight vector.

Data

By mining and analyzing the geologic and hydrogeologic data of the Xiaojihan Mine throughout its exploration, well construction, and production phases, 103 valid boreholes records have been obtained for 11th and 13th panels. The evaluation criteria for the water abundance of the J_2z–$^{\#}2$ coal seam roof fissured aquifer have been determined. These criteria include the aquifer thickness, ratio of brittle and plastic rock, core recovery rate, specific capacity, and hydraulic conductivity. The data associated with these criteria were derived from 103 boreholes, 103 boreholes, 103 boreholes, 7 boreholes, and 7 boreholes, respectively.

Results and Discussion

Thematic Maps

Aquifer Thickness

In certain conditions, a thicker aquifer indicates a stronger water abundance. The J_2z–$^{\#}2$ coal seam roof fissured aquifer in the 11th and 13th panels consists of fine sandstone, medium sandstone, and coarse sandstone layers. The combined thickness, from the J_2z to the top of the $^{\#}2$ coal seam in the borehole, is considered the total thickness of the aquifer. The total thickness of the J_2z–$^{\#}2$ coal seam roof fissured aquifer ranges from 20.85 m to 155.29 m, with an average thickness of 69.32 m, exhibiting a general trend of thinning from west to east (Fig. 4).

The Ratio of Brittle and Plastic Rock

Mudstone generally exhibits water-blocking properties. The thickness of fine, medium, and coarse sandstone from the J_2z to the top of the $^{\#}2$ coal seam represents the brittle rock thickness, while the mudstone thickness represents the plastic rock thickness. A higher proportion of brittle and plastic rocks indicates a greater water abundance of the aquifer. The thickness ratio of brittle and plastic rock from the J_2z to the top of the $^{\#}2$ coal seam in the 11th and

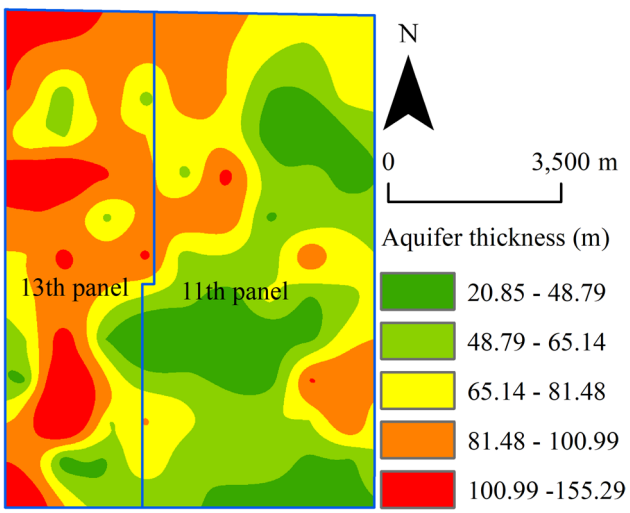

Fig. 4 Thematic maps of aquifer thickness

13th panels ranges from 0 to 18.44, with an average of 3.14 m. The mudstone strata in the western and northeastern regions are thin or absent, leading to a higher thickness ratio of brittle and plastic rock (Fig. 5).

The Core Recovery Rate

The core recovery rate is the ratio of the core length to the footage during boreholes and is an indication of the rock mass integrity. Typically, a lower core recovery rate indicates a more fragmented rock mass and greater water abundance. The core recovery rate of boreholes in the 11th and 13th panels was generally high, ranging from 60.99 to 97.05% with an average of 80.91%. Based on the map of the core recovery rate (Fig. 6), the western and southeastern part of the region had a low core recovery rate, indicating a relatively fragmented rock.

The Specific Capacity

The borehole specific capacity refers to the volume of water discharged during a pumping test when the well water level decreases by one meter. It is an important parameter for assessing the water abundance of an aquifer. Generally, a higher specific capacity indicates greater water abundance within the aquifer. The specific capacity from the J_2z to the top of the $^{\#}2$ coal seam in the 11th and 13th panels ranges from 0.012 L/(s·m) to 0.044 L/(s·m), averaging 0.034 L/(s·m). Based on the map of borehole specific capacity, there is a general decrease from east to west (Fig. 7).

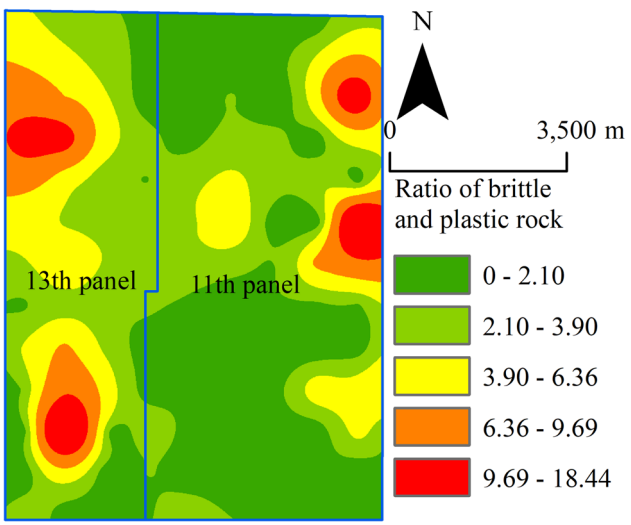

Fig. 5 Thematic map of ratio of brittle and plastic rock

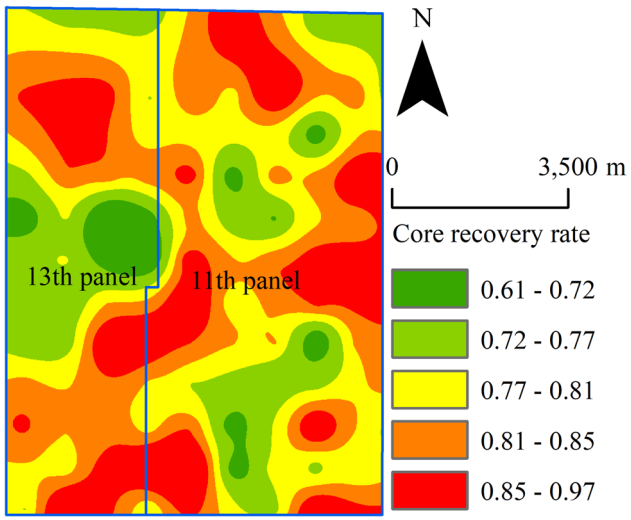

Fig. 6 Thematic map of core recovery ratio

The Hydraulic Conductivity

The hydraulic conductivity serves as a widely used parameter for assessing the permeability of rock strata. Generally, a higher hydraulic conductivity indicates greater water abundance. The hydraulic conductivity from the J_2z to the top of the $^{\#}2$ coal seam in the 11th and 13th panels ranging from 0.0014 m/d to 0.0651 m/d with an average of 0.0266 m/d. Based on the map of the hydraulic conductivity (Fig. 8), distinct boundaries can be observed. The hydraulic conductivity in the northeast is larger, the boundary is the most prominent, and the hydraulic conductivity in the southeast is relatively small.

The data of the five evaluation indexes are standardized and made dimensionless using either the maximum or the

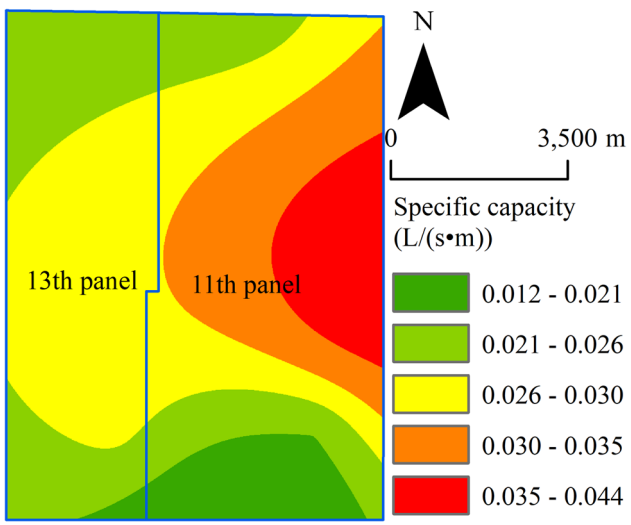

Fig. 7 Thematic maps of specific capacity

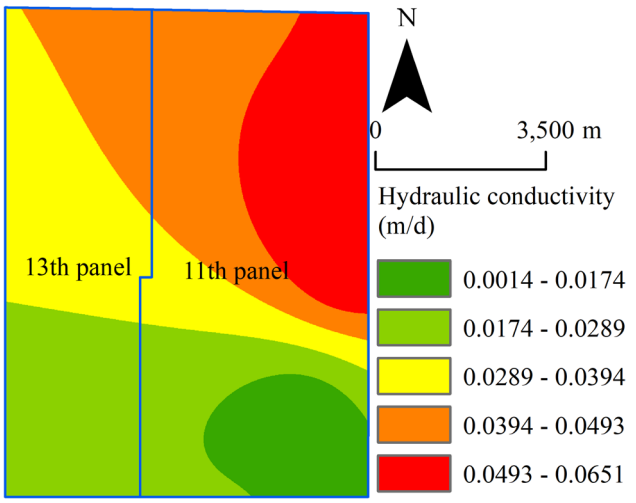

Fig. 8 Thematic maps of hydraulic conductivity

Table 2 Weights of the main influencing factors

The main influencing factors	The aquifer thickness	The core recovery rate	The ratio of brittle and plastic rock	The borehole specific capacity	The hydraulic conductivity
Weight	0.2702	0.0801	0.0801	0.3418	0.2279

minimum value method. ArcGIS software is employed to establish thematic layers for each evaluation index, which form the foundation for multisource information fusion.

Water Abundance Evaluation Based on Constant Weight

The AHP method is employed to determine the constant weights of the five main influencing factors (Table 2). The consistency test demonstrated a CI value below 0.1. The water abundance index, based on the constant weights, is calculated using Eq. 6. ArcGIS is used to draw the water abundance zoning map of the $J_2z - {}^{\#}2$ coal seam roof fissured aquifer. The water abundance index data is classified into five levels using the Jenks natural breaks method (Zeng et al. 2017). Figure 9a illustrates the results. Strong water abundance areas are primarily concentrated in the central, eastern, and southwestern parts of the study area, while weak water abundance areas are concentrated in the southern region. It is important to note that the relative water abundance reflects the relative strength of water abundance in the study area, rather than its absolute degree.

Water abundance Evaluation Based on Variable Weight

The AHP is initially employed to calculate the constant weights for each main influencing factor. Based on the determined constant weights, the K-means clustering method is applied to divide the weight adjustment interval, calculate the interval threshold, and determine the variable weight interval for each main influencing factor (Table 3). The evaluation unit that satisfies the constraints is selected to construct the ideal variable weight, and the corresponding parameter values of the variable weight model are calculated (Table 4). Finally, the variable weight combination of evaluation indexes at different coordinate points in the study area is calculated using MATLAB software, and selected weight values are presented in Table 5.

The variable weight model calculates the weight combination, which is then used to calculate the water abundance index based on Eq. (12). Subsequently, all water abundance index data are classified into five levels using the Natural Jenks method (Fig. 9b).

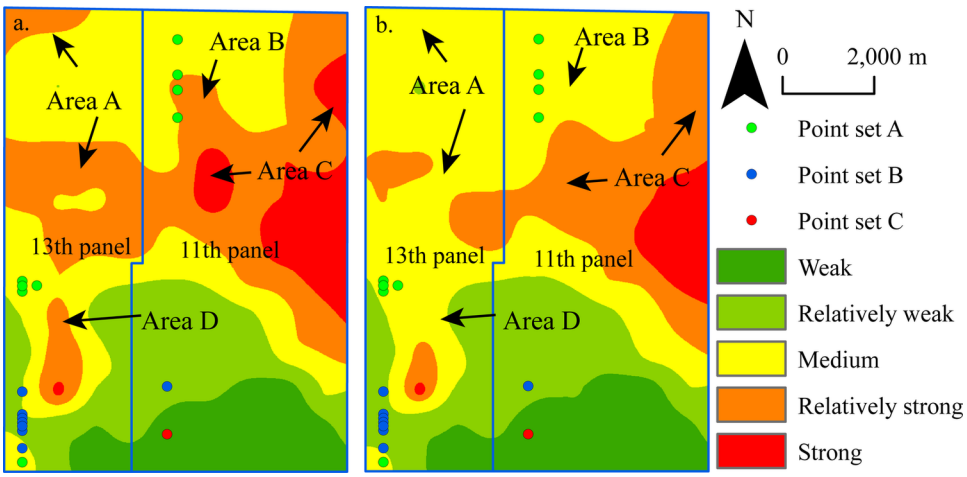

Fig. 9 Water-abundance zoning map of the $J_2z–{}^{\#}2$ coal seam roof fissure aquifer: **a** constant weight model, **b** variable weight model

Table 3 Variable weight interval of the main influencing factors

The main influencing factors	The property of variable weight interval			
	The punishment interval	The invariant interval	The initial incentive interval	The strong incentive interval
The aquifer thickness	$0 \le x < 0.2151$	$0.2151 \le x < 0.4266$	$0.4266 \le x < 0.7236$	$0.7236 \le x \le 1$
The ratio of brittle and plastic rock	$0 \le x < 0.1522$	$0.1522 \le x < 0.4450$	$0.4450 \le x < 0.8316$	$0.8316 \le x \le 1$
The core recovery rate	$0 \le x < 0.3006$	$0.3006 \le x < 0.4894$	$0.4894 \le x < 0.7032$	$0.7032 \le x \le 1$
The specific capacity	$0 \le x < 0.0833$	$0.0833 \le x < 0.3333$	$0.3333 \le x < 0.7576$	$0.7576 \le x \le 1$
The hydraulic conductivity	$0 \le x < 0.1806$	$0.1806 \le x < 0.5056$	$0.5056 \le x < 0.8462$	$0.8462 \le x \le 1$

Table 4 Variable weight model parameter values

Variable weight parameter	k_1	k_2	k_3	c	a_1	a_2	a_3
Parameter value	− 0.0596	− 0.2998	3.6758	0.0553	− 0.2426	0.0105	− 1.9524

Comparative Verification

The water abundance zoning map based on constant weight and variable weight is verified using the collected water exploration and drainage data. The analysis reveals that 10 boreholes (point set A) with drainage volumes ranging from 0.93 to 1.9 m^3/h are situated in the medium water abundance area, while seven boreholes (point set B) with drainage volumes ranging from 0.39 to 0.88 m^3/h are located in the relatively weak water abundance area. Additionally, one borehole (point set C) with a drainage volume of 0.25 m^3/h is found in the weak water abundance area (Fig. 9b). These findings align with the results of water abundance zoning based on variable weight, demonstrating a 100% degree of agreement. Out of the collected water exploration and drainage data, three borehole (point set A) drainage records did not align with the water abundance zoning results based on constant weight, resulting in an 83% coincidence rate (Fig. 9a). This indicates that the water abundance zoning results based on the variable weight model are more accurate and better reflect the aquifer's actual water abundance.

The evaluation results of the J_2z–$^{\#}2$ coal seam roof fissured aquifer were compared using both the traditional constant weight model and the variable weight model. Overall, the evaluation results exhibit a consistent trend, but variations exist in specific local areas (areas A, B, C, and D on the zoning map). For instance, in area A, the water abundance of the J_2z–$^{\#}2$ coal seam roof fissured aquifer transitions from a relatively strong water-abundance area in the constant weight model to a medium water-abundance area in the variable weight model. This difference can be attributed to the low specific capacity of the borehole in the aquifer and the low ratio of brittle and plastic rock in this area. Consequently, compared to other significant influencing factors, these two factors exert a stronger influence on the water abundance of the region. Strengthening their weight effectively emphasizes their control in evaluating water abundance, resulting in more realistic evaluation results.

Figure 9b illustrates a clear pattern of decreasing water abundance in the J_2z–$^{\#}2$ coal seam roof fissured aquifer at the Xiaojihan coal mine, both from east to west and from north to south. The distribution of water-abundant areas in the aquifer is uneven. The strong and relatively strong water abundant areas are primarily concentrated in the eastern part of the 11th panel, with scattered occurrences in the 13th panel. The medium water abundant areas are found in the central regions of the 13th and 11th panel, while the remaining areas exhibit weak and relatively weak water abundance. As the sole aquifer directly supplying water to the $^{\#}2$ coal seam in the Xiaojihan Mine, the water abundance of the J_2z–$^{\#}2$ coal seam roof fissured aquifer serves as a direct indicator of the water-related risks in the $^{\#}2$ coal mining. Consequently, we recommend intensifying groundwater-level monitoring and closely monitoring water inflow in working faces located in water abundant and highly water abundant regions to prevent water-related accidents. In addition, prior to commencing mining operations in water abundant and highly water abundant regions, it is essential to implement advanced drainage measures to proactively reduce water inflow.

Conclusion

We propose a method for calculating the aquifer water abundance index using a variable weight model. By systematically analyzing the lithological characters, hydraulic characteristics, geologic structural factors, and geophysical parameters of the aquifer, we constructed a comprehensive system of four major categories and 16 sub-categories of

Table 5 Partial variable weight values of the main influencing factors

The aquifer thickness (m)	Weight	The ratio of brittle and plastic rock	Weight	The core recovery rate	Weight	The specific capacity L/(s·m)	Weight	The hydraulic conductivity (m/d)	Weight
0.1914	0.2487	0.2208	0.2382	0.3199	0.3573	0.2881	0.0785	0.0671	0.0772
0.1921	0.2487	0.2206	0.2382	0.3208	0.3573	0.2898	0.0785	0.0671	0.0772
0.1928	0.2488	0.2204	0.2382	0.3216	0.3573	0.2915	0.0786	0.0671	0.0772
0.1935	0.2488	0.2202	0.2382	0.3224	0.3572	0.2933	0.0786	0.0670	0.0772
0.1942	0.2488	0.2199	0.2382	0.3232	0.3572	0.2951	0.0786	0.0670	0.0772
0.1950	0.2488	0.2197	0.2382	0.3241	0.3572	0.2969	0.0786	0.0671	0.0772
0.1957	0.2489	0.2195	0.2381	0.3249	0.3571	0.2987	0.0787	0.0671	0.0772
0.1965	0.2489	0.2193	0.2381	0.3257	0.3571	0.3005	0.0787	0.0671	0.0772
0.1973	0.2489	0.2191	0.2381	0.3266	0.3571	0.3024	0.0787	0.0671	0.0772
0.1981	0.2490	0.2189	0.2381	0.3274	0.3571	0.3043	0.0787	0.0671	0.0772
0.1989	0.2490	0.2187	0.2381	0.3282	0.3571	0.3062	0.0787	0.0671	0.0772
0.1997	0.2490	0.2185	0.2381	0.3291	0.3571	0.3081	0.0787	0.0671	0.0772
0.2006	0.2491	0.2183	0.2381	0.3299	0.3570	0.3101	0.0787	0.0671	0.0772
0.2015	0.2491	0.2181	0.2380	0.3308	0.3570	0.3121	0.0787	0.0672	0.0772
0.2023	0.2491	0.2179	0.2380	0.3317	0.3570	0.3140	0.0787	0.0672	0.0771
0.2032	0.2492	0.2177	0.2380	0.3325	0.3570	0.3161	0.0787	0.0672	0.0771
0.2041	0.2492	0.2175	0.2380	0.3334	0.3570	0.3181	0.0787	0.0672	0.0771
0.2051	0.2493	0.2173	0.2380	0.3343	0.3569	0.3201	0.0787	0.0673	0.0771
0.2060	0.2493	0.2171	0.2380	0.3351	0.3569	0.3222	0.0787	0.0673	0.0771
0.2070	0.2493	0.2169	0.2380	0.3360	0.3569	0.3243	0.0787	0.0673	0.0771
0.2079	0.2494	0.2167	0.2380	0.3369	0.3569	0.3264	0.0787	0.0674	0.0771
0.2089	0.2494	0.2166	0.2380	0.3378	0.3568	0.3285	0.0787	0.0674	0.0771
0.2099	0.2495	0.2164	0.2380	0.3387	0.3568	0.3307	0.0786	0.0675	0.0771
0.2110	0.2495	0.2162	0.2379	0.3396	0.3568	0.3328	0.0786	0.0675	0.0771
0.2120	0.2496	0.2160	0.2379	0.3404	0.3567	0.3350	0.0786	0.0676	0.0771
0.2131	0.2496	0.2159	0.2379	0.3413	0.3567	0.3372	0.0786	0.0677	0.0771
0.2142	0.2497	0.2157	0.2379	0.3422	0.3567	0.3395	0.0786	0.0677	0.0771
0.2153	0.2497	0.2155	0.2379	0.3432	0.3566	0.3417	0.0786	0.0678	0.0771
0.2164	0.2497	0.2154	0.2379	0.3441	0.3566	0.3439	0.0786	0.0679	0.0771
0.2175	0.2497	0.2152	0.2379	0.3450	0.3566	0.3462	0.0786	0.0679	0.0771
0.2186	0.2497	0.2151	0.2379	0.3459	0.3566	0.3485	0.0786	0.0680	0.0771
0.2198	0.2497	0.2149	0.2379	0.3468	0.3566	0.3508	0.0786	0.0681	0.0771
0.2210	0.2497	0.2148	0.2379	0.3477	0.3566	0.3531	0.0786	0.0682	0.0771
0.2222	0.2497	0.2146	0.2379	0.3487	0.3566	0.3555	0.0786	0.0683	0.0771
0.2234	0.2497	0.2145	0.2379	0.3496	0.3566	0.3578	0.0786	0.0684	0.0771
0.2247	0.2497	0.2143	0.2379	0.3505	0.3566	0.3602	0.0786	0.0685	0.0771
0.2259	0.2497	0.2142	0.2379	0.3514	0.3566	0.3626	0.0786	0.0686	0.0771
0.2272	0.2497	0.2141	0.2379	0.3524	0.3565	0.3649	0.0786	0.0687	0.0771
0.2285	0.2498	0.2139	0.2379	0.3533	0.3565	0.3674	0.0786	0.0689	0.0771
0.2298	0.2498	0.2138	0.2379	0.3543	0.3565	0.3698	0.0786	0.0690	0.0771
0.2312	0.2498	0.2137	0.2379	0.3552	0.3565	0.3722	0.0786	0.0691	0.0772
0.2325	0.2498	0.2136	0.2379	0.3562	0.3565	0.3746	0.0786	0.0693	0.0772
0.2339	0.2498	0.2135	0.2379	0.3571	0.3565	0.3771	0.0786	0.0694	0.0772
0.2353	0.2498	0.2134	0.2379	0.3581	0.3565	0.3795	0.0786	0.0696	0.0772
0.2367	0.2498	0.2133	0.2379	0.3591	0.3565	0.3820	0.0786	0.0697	0.0772
0.2381	0.2498	0.2132	0.2379	0.3600	0.3565	0.3845	0.0786	0.0699	0.0772
0.2396	0.2498	0.2131	0.2380	0.3610	0.3565	0.3870	0.0786	0.0700	0.0772
0.2410	0.2498	0.2130	0.2380	0.3620	0.3564	0.3895	0.0787	0.0702	0.0772
0.2425	0.2498	0.2129	0.2380	0.3630	0.3564	0.3920	0.0787	0.0704	0.0772

Table 5 (continued)

The aquifer thickness (m)	Weight	The ratio of brittle and plastic rock	Weight	The core recovery rate	Weight	The specific capacity L/(s·m)	Weight	The hydraulic conductivity (m/d)	Weight
0.2440	0.2498	0.2128	0.2380	0.3639	0.3564	0.3945	0.0787	0.0706	0.0772
0.2455	0.2498	0.2127	0.2380	0.3649	0.3564	0.3970	0.0787	0.0708	0.0772
0.2470	0.2498	0.2127	0.2380	0.3659	0.3564	0.3995	0.0787	0.0710	0.0772
0.2486	0.2498	0.2126	0.2380	0.3669	0.3564	0.4020	0.0787	0.0712	0.0772
0.2501	0.2498	0.2125	0.2380	0.3679	0.3564	0.4045	0.0787	0.0714	0.0772
0.2517	0.2498	0.2125	0.2380	0.3689	0.3564	0.4070	0.0787	0.0716	0.0772
0.2533	0.2498	0.2124	0.2380	0.3699	0.3564	0.4095	0.0787	0.0719	0.0772
0.2549	0.2498	0.2124	0.2380	0.3709	0.3563	0.4121	0.0787	0.0721	0.0772
0.2565	0.2498	0.2123	0.2380	0.3719	0.3563	0.4146	0.0787	0.0724	0.0772
0.2581	0.2498	0.2123	0.2380	0.3729	0.3563	0.4171	0.0787	0.0726	0.0772

primary influencing factors that describe the distribution pattern of water abundance areas in the aquifer. We introduced standardization and dimensionless processing methods for the main influencing factor index values, which provide a foundation for researching a multisource information fusion model. We outlined the steps for determining the variable weights of the primary influencing factors in different states and constructed the water abundance index model based on the variable weight theory.

The enhanced water abundance index method further improves the evaluation results for water abundance. The variable weight model is used to optimize the weights by considering the state values and combined values of various parameters at different locations within the study area. The variable weight model addresses the limitations of applying the same weight across the entire study area. The enhanced model exhibits higher dispersity and yields more reasonable and accurate results, highlighting the impact of weight variations for each parameter on the evaluation of water abundance.

By applying this new method in the Xiaojihan coal mine, we discovered a decreasing trend in the water abundance intensity of the direct water-filled J_2z–$^{\#}2$ coal seam roof fissured aquifer, moving from east to west and from north to south. The areas with strong and relatively strong water abundance are primarily concentrated in the eastern part of the 11th panel, with sporadic distribution also observed in the 13th panel. We recommend enhanced monitoring of groundwater levels and water inflow in the working face to prevent water-related accidents when mining these areas.

Acknowledgements This research was financially supported by the China National Natural Science Foundation (42027801, 42072284, 42372297), the National Key R&D Program of China (2023YFC3012102, 2021YFC2902004), and the Fundamental Research Funds for the Central Universities (2023ZKPYSH01). The authors also thank the editor and reviewers for their constructive suggestions.

Funding China National Natural Science Foundation, 42027801, Qiang Wu, 42072284, Yifan Zeng, 42372297, Yifan Zeng, National Key R&D Program of China, 2023YFC3012102, Yifan Zeng, 2021YFC2902004, Fundamental Research Funds for the Central Universities, 2023ZKPYSH01.

Data availability The authors do not have permission to share data.

References

Gui HR, Lin ML (2016) Types of water hazards in China coalmines and regional characteristics. Nat Hazards 84:1501–1512. https://doi.org/10.1007/s11069-016-2488-5

Han C, Pan X, Li G, Tu J (2012) The Fuzzy analytic hierarchy process of water abundance of an aquifer based on GIS and multi-source information fusion techniques. Hydrogeol Eng Geol 39:19–25. https://doi.org/10.16030/j.cnki.issn.1000-3665.2012.04.012. (**In Chinese**)

He X, Duan Z, Miao L, Zhang J (2019) Unconfined aquifer water-richness and dynamic change features of Mu Us Desert area in northern Shaanxi. J xi'an Univ Sci Technol 39:88–95. https://doi.org/10.13800/j.cnki.xakjdxxb.2019.0113. (**In Chinese**)

Hou E, Yan X, Zheng Y, Yang F (2019) Application of Bayes discriminant model in prediction of water enrichment of weathered bedrock. J xi'an Univ Sci Tech 39:942–949. https://doi.org/10.13800/j.cnki.xakjdxxb.2019.0604. (**In Chinese**)

Li XF (2010) Water abundance forecast and water disaster danger evaluation study of sandstone aquifers. MS Thesis, Shandong Univ, People's Republic of China

Li D-q, Hao F-l (2009) Weights transferring effect of state variable weight vector. Syst Eng Theory Pract 29:127–131. https://doi.org/10.1016/S1874-8651(10)60054-3

Li LN, Li WP, Shi SQ, Yang Z, He JH, Chen WC, Yang YR, Zhu TG, Wang QQ (2022a) An improved potential groundwater yield zonation method for sandstone aquifers and its application in Ningxia, China. Nat Resour Res 31:849–865. https://doi.org/10.1007/s11053-022-10021-2

Li LN, Li WP, Wang QQ (2022b) Prediction and zoning of the impact of underground coal mining on groundwater resources. Process Saf Environ Prot 168:454–462. https://doi.org/10.1016/j.psep.2022.10.013

Mei AS, Wu Q, Zeng YF, Cui YS, Zhao D (2023) Evaluation of water inrush vulnerability and feasibility analysis of mining under rivers:

a case study involving the Jinjie coal mine in China. Mine Water Environ 42:312–329. https://doi.org/10.1007/s10230-023-00939-1

Mu W, Wu X, Ding H, Geng F, Yu S, Zhang X (2022) A hydro-economic model for optimizing management of mine water: a case study in the Suancigou coal mine, northwestern China. Mine Water Environ. https://doi.org/10.1007/s10230-022-00894-3

National Coal Mine Safety Administration (2018) Coal Mine Water Control Rules. China Coal Industry Publishing House, Beijing, China

Pang K, Wu Q, Zeng Y (2022) Prediction of roof water inrush risk under the complex condition of interbedded aquifer and multi burnt rock aquifers. Coal Eng 54:135–141 ((**in Chinese**))

Qu XY, Han J, Shi LQ, Qu XW, Bilal A, Qiu M, Gao WF (2023) An extended ITL-VIKOR model using triangular fuzzy numbers for applications to water-richness evaluation. Expert Syst Appl 222:13. https://doi.org/10.1016/j.eswa.2023.119793

Saaty TL (1990) How to make a decision: the analytic hierarchy process. Eur J Oper Res 48:9–26. https://doi.org/10.1016/0377-2217(90)90057-i

Wang P (1985) Shadow of fuzzy sets and random sets. Beijing Normal University Press, Beijing, China

Wang SS (2011) Evaluation of the ordovician limestone water enrichment and water inrush risks of the no.11 coal seam floor in baode coal mine. MS Thesis. Shandong Univ, People's Republic of China

Wang M-W, Xu P, Li J, Zhao K-Y (2014) A novel set pair analysis method based on variable weights for liquefaction evaluation. Nat Hazards 70:1527–1534. https://doi.org/10.1007/s11069-013-0887-4

Wu Q, Fan ZL, Zhang ZW, Zhou WF (2014) Evaluation and zoning of groundwater hazards in Pingshuo no. 1 underground coal mine, Shanxi Province. China Hydrogeol J 22:1693–1705. https://doi.org/10.1007/s10040-014-1138-9

Wu Q, Liu Y, Luo L, Liu S, Sun W, Zeng Y (2015a) Quantitative evaluation and prediction of water inrush vulnerability from aquifers overlying coal seams in Donghuantuo coal mine, China. Environ Earth Sci 74:1429–1437. https://doi.org/10.1007/s12665-015-4132-1

Wu Q, Liu Y, Zhou W, Wu X, Liu S, Sun W, Zeng Y (2015b) Assessment of water inrush vulnerability from overlying aquifer using GIS-AHP-based "three maps-two predictions" method: a case study in Hulusu coal mine, China. Q J Eng Geol Hydrogeol 48:234–243. https://doi.org/10.1144/qjegh2015-014

Wu Q, Liu YZ, Zhou WF, Li BY, Zhao B, Liu SQ, Sun WJ, Zeng YF (2015c) Evaluation of water inrush vulnerability from aquifers overlying coal seams in the Menkeqing coal mine, China. Mine Water Environ 34:258–269. https://doi.org/10.1007/s10230-014-0313-5

Xiao L, Niu C, Dai G, Nie W, Zhang H, Gao Y (2018) Evaluation of water abundance in Zhiluo formation based watery structure index method. Coal Sci Technol 46:207–213. https://doi.org/10.13199/j.cnki.cst.2018.11.032. (**In Chinese**)

Xue J (2020) Application of water-rich index method based on fractal theory in water-rich evaluation of aquifer. Safety Coal Mines 51:197–201. https://doi.org/10.13347/j.cnki.mkaq.2020.02.044. (**In Chinese**)

Yu H, Wu Q, Zeng Y, Zheng L, Xu L, Liu S, Wang D (2022) Integrated variable weight model and improved DRASTIC model for groundwater vulnerability assessment in a shallow porous aquifer. J Hydrol. https://doi.org/10.1016/j.jhydrol.2022.127538

Zeng Y (2018) Research on Risk Evaluation Methods of Groundwater Bursting from Aquifers Underlying Coal Seams and Applications to Coalfields of North China. Springer International Publishing, Cham

Zeng Y, Wu Q, Liu S, Zhai Y, Lian H, Zhang W (2017) Evaluation of a coal seam roof water inrush: case study in the Wangjialing coal mine, China. Mine Water Environ 37:174–184. https://doi.org/10.1007/s10230-017-0459-z

Zeng YF, Lian HQ, Du X, Tan XF, Liu DM (2022) An analog model study on water-sand mixture inrush mechanisms during the mining of shallow coal seams. Mine Water Environ 41:428–436. https://doi.org/10.1007/s10230-022-00870-x

Zhang C, Yue N, Li S, Yan G, Liu S, Yang Z (2019) Multiple information prediction and evaluation of water yield property for bedrock aquifer. Safety Coal Mines 50:196–199. https://doi.org/10.13347/j.cnki.mkaq.2019.11.046